F. L. Paton, H. R. Maier, and G. C. Dandy

Including adaptation and mitigation responses to climate change in a multiobjective evolutionary algorithm framework for urban water supply systems incorporating GHG emissions

Water Resources Research, 2014; 50(8):6285-6304

DOI: http://dx.doi.org/10.1002/2013WR015195

AGU PUBLICATIONS

Water Resources Research

RESEARCH ARTICLE
10.1002/2013WR015195

Key Points:
- Developing an urban water supply planning framework to mitigate GHG emissions
- Analyzing the impact of minimizing GHG emissions on cost and supply security
- Using a real-life case study to illustrate the planning value of the approach

Supporting Information:
- Readme
- Text 1
- Text 2
- Figure S1
- Figure S2
- Figure S3
- Figure S4

Correspondence to:
F. L. Paton,
fpaton@civeng.adelaide.edu.au

Citation:
Paton, F. L., H. R. Maier, and G. C. Dandy (2014), Including adaptation and mitigation responses to climate change in a multiobjective evolutionary algorithm framework for urban water supply systems incorporating GHG emissions, *Water Resour. Res.*, *50*, 6285–6304, doi:10.1002/2013WR015195.

Received 18 DEC 2013
Accepted 8 JUL 2014
Accepted article online 10 JUL 2014
Published online 4 AUG 2014

Including adaptation and mitigation responses to climate change in a multiobjective evolutionary algorithm framework for urban water supply systems incorporating GHG emissions

F. L. Paton[1], H. R. Maier[1], and G. C. Dandy[1]

[1]School of Civil, Environmental and Mining Engineering, University of Adelaide, Adelaide, South Australia, Australia

Abstract Cities around the world are increasingly involved in climate action and mitigating greenhouse gas (GHG) emissions. However, in the context of responding to climate pressures in the water sector, very few studies have investigated the impacts of changing water use on GHG emissions, even though water resource adaptation often requires greater energy use. Consequently, reducing GHG emissions, and thus focusing on both mitigation and adaptation responses to climate change in planning and managing urban water supply systems, is necessary. Furthermore, the minimization of GHG emissions is likely to conflict with other objectives. Thus, applying a multiobjective evolutionary algorithm (MOEA), which can evolve an approximation of entire trade-off (Pareto) fronts of multiple objectives in a single run, would be beneficial. Consequently, the main aim of this paper is to incorporate GHG emissions into a MOEA framework to take into consideration both adaptation and mitigation responses to climate change for a city's water supply system. The approach is applied to a case study based on Adelaide's southern water supply system to demonstrate the framework's practical management implications. Results indicate that trade-offs exist between GHG emissions and risk-based performance, as well as GHG emissions and economic cost. Solutions containing rainwater tanks are expensive, while GHG emissions greatly increase with increased desalinated water supply. Consequently, while desalination plants may be good adaptation options to climate change due to their climate-independence, rainwater may be a better mitigation response, albeit more expensive.

1. Introduction

Cities around the world are increasingly engaged in climate action and mitigating greenhouse gas (GHG) emissions [*Miller et al*., 2013; *National Research Council*, 2009]. However, *Rothausen and Conway* [2011] conclude that energy use and GHG emissions associated with water management are poorly understood and have only been partially considered in water resources management. Consequently, the consideration of GHG emissions in the water sector is both timely and necessary, particularly because of: (1) the high sensitivity of the water sector to climate change [*Rothausen and Conway*, 2011]; and (2) the close link between water and energy [*Stokes and Horvath*, 2009; *Stokes et al*., 2014], often referred to as the water-energy nexus and referencing the use of water in many processes of electricity generation, as well as the use of energy in water supply and wastewater treatment [*Miller et al*., 2013]. In addition, energy and carbon use in the water sector is both intensive [*Roshani et al*., 2012] and increasing [*Rothausen and Conway*, 2011].

The trend of increasing energy use in the water sector is expected to continue, because as *Rothausen and Conway* [2011] note, water resource adaptation will often mean that more energy is required to meet rising demand, regulatory standards and the effects of climate change. For example, some adaptation options to climate change, such as desalination and pumping, are very energy intensive. This means that GHG emissions are also likely to rise, given the extensive use of nonrenewable sources, such as fossil fuels, to produce energy around the world. It is therefore concerning that, water resource adaptation will most likely increase GHG emissions, given that: (a) GHG emissions contribute to climate change; (b) climate change will in many places exacerbate water scarcity; and (c) water scarcity is a driver for water resource adaptation. Consequently, reducing GHG emissions, and focusing on both mitigation and adaptation responses to climate change in planning and managing urban water supply systems, is necessary.

While the consideration of GHG emissions from urban water supply systems is both timely and necessary, the minimization of GHG emissions is likely to conflict with other objectives, such as maximizing water supply security. Thus, multiple objectives will need to be balanced and negotiated [*Reed et al*., 2003]. Balancing such objectives can be greatly aided by the application of multiobjective evolutionary algorithms (MOEAs) because they can rapidly evolve an approximation of entire trade-off (Pareto) fronts of multiple objectives in a single run [*Reed et al*., 2003].

In recent years, a number of MOEA studies concerned with the design and operation of water distribution systems have considered GHG emissions reduction as one of the objectives [*Stokes et al*., 2014; *Wu et al*., 2009, 2010, 2013, 2012], or as a component of a broader environmental objective [*Herstein et al*., 2009, 2011; *Herstein and Filion*, 2011]. Similarly, *Roshani et al*. [2012] examined the cost of GHG emissions (that is the cost associated with a carbon price levied on electricity used for pumping water) as a component of total system costs for a water distribution network expansion in a single-objective, evolutionary algorithm optimization problem. However, this focus on water supply infrastructure ignores a number of important issues related to the minimization of GHG emissions from urban water supply systems, such as in assessing alternative water supply sources (e.g., desalination plants) that may be introduced as adaptation responses to climate change for a city's water supply system. Consequently, there is a need to explore the optimal trade-offs between GHG emissions and other objectives, such as minimizing cost and maximizing water supply security, for urban water supply systems at the regional scale.

A number of studies have examined GHG emissions of regional-scale urban water supply systems [*Barjoveanu et al*., 2014; *Lundie et al*., 2004; *Sahely et al*., 2005; *Sahely and Kennedy*, 2007; *Stokes and Hovarth*, 2006; *Slagstad and Brattebø*, 2014]. However, while these studies thoroughly explore GHG emissions from an environmental impact perspective, they do not include multiobjective optimization, let alone a MOEA. In fact, of the MOEA studies that have focused on regional scale water supply system management and planning, none has considered GHG emissions reduction as an objective [*Kasprzyk et al*., 2009, 2012, 2013; *Mortazavi et al*., 2012]. Consequently, in order to address this shortcoming, the main aim of this paper is to develop a MOEA framework for urban water supply systems that takes into consideration both adaptation and mitigation responses to climate change. The specific objectives are: (1) to use GHG emissions as an objective function and to include both mitigation and adaptation options to climate change in a MOEA framework for urban water supply systems at the regional scale; (2) to evaluate the implications of optimizing for GHG emissions on economic cost and water supply system security; and (3) to demonstrate practical management implications of the framework by applying it to a case study based on Adelaide's southern water supply system. While the approach is applied to a case study, its generic nature means it could be readily applied to other city's water supply systems around the world.

The remainder of this paper is organized as follows. In section 2, the issues and challenges of incorporating GHG emissions into multiobjective optimization of regional water supply systems are highlighted. The case study is then introduced in section 3, followed by a description of the MOEA framework applied to the case study to demonstrate the value of the approach (section 4). The results are discussed in section 5. Section 6 summarizes the paper, focusing on the key conclusions drawn.

2. Incorporation of GHG Emissions in the Multiobjective Optimization of Regional Water Supply Systems

As mentioned in section 1, the adaptation of city water supply systems to climate change can often lead to an increase in energy and GHG emissions, which thus conflicts with any aims by the water sector to mitigate climate change. Therefore, to balance adaptation to and mitigation of climate change, it is not only necessary to estimate how well solutions perform under future climate change conditions (i.e., adaptation), but also the quantity of GHG emissions that are associated with each solution (i.e., mitigation). Furthermore, given that there are (1) other objectives to consider, such as economic cost, and (2) a great number of potential solutions, there is a compelling argument for applying multiobjective optimization of regional water supply systems incorporating GHG emissions. However, this is not a straightforward task.

The first difficulty for modelers is the issue of how to evaluate GHG emissions, particularly given the uncertainty in estimating the quantity of emissions that are created by any given process. In accounting for GHG emissions of an urban water supply system, operational GHG emissions need to be estimated for existing

supply sources, and both capital and operational GHG emissions need to be estimated for new supply sources. However, GHG emissions data specific to supply sources may not be readily available (particularly for nontraditional sources, such as storm water harvesting). Furthermore, if these data were available, they may be heavily dependent on local conditions (e.g., the rate of emissions), so transferring data from a case study in one city to another may be inappropriate. To overcome this problem, capital emissions for supply sources can be derived from embodied energy of material use, while operating emissions for supply sources can be derived from annual energy consumption [*Wu et al*., 2010]. However, the modeler then faces the issue of estimating energy use and selecting an appropriate emission factor (tonnes of CO_2 equivalent emissions per megawatt hour of electricity generated), which will be heavily dependent on the fuel mix used: electricity generated predominantly from fossil fuels will have a much higher emission factor than electricity generated from renewable sources, such as wind energy. Furthermore, the sources of electricity for a particular city may vary in time and space, so more detailed, coupled modeling studies that include electricity generation may thus be required to increase our understanding of this topic in the future [*Stokes et al*., 2014].

There is also the issue of whether GHG emissions estimated to occur in the future should be discounted. *Wu et al*. [2010] explain that a discount rate of zero (i.e., no discounting) is very often used for GHG impact evaluation, reflecting the notion that future GHG emissions do not have a lower impact than emissions at the current time. However, a positive discount rate may be appropriate for GHG emissions if, for example, technology advancement can significantly reduce the cost of GHG abatement or carbon sequestration in the future [*Wu et al*., 2010] or one takes into account that all GHG emissions undergo natural decay in the atmosphere. If so, then as is the case with discounting economic costs, a decision must be made as to what is an appropriate discount rate to apply. For economic costs, high discount rates match the prevailing rates in the private sector but discourage investment in long-term conservation of natural resources; while low discount rates, which are less likely to be justified economically, are set to favor long-term environmental conservation projects [*Cai et al*., 2002]. On the contrary, when discounting GHG emissions of water supply systems, the application of a positive discount rate, particularly a high discount rate, will favor sources with high operational emissions and lower embodied energy (such as desalination plants), because the future GHG emissions will be discounted, thus reducing the total GHG emissions of these sources.

Finally, GHG emissions or energy data might not be readily available, or easy to estimate, for all components of a water supply system. Consequently, modelers may have to work with imperfect GHG emissions data for some supply sources, until further research into energy and/or GHG emissions for such water supply sources occurs.

3. Case Study: The Southern Adelaide System

With a population of about 1.2 million people, the capital city of South Australia—Adelaide (Figure 1), has an average water demand over the past 20 years of about 200 gigaliters per year (GL/yr) [*Government of South Australia*, 2009]. However, this case study focuses on Adelaide's southern water supply system, which supplies approximately half of Adelaide's demand, with an indicative demand area illustrated in Figure 1. Furthermore, in the case study, the current system refers to Adelaide's southern water supply system as it was in 2009, which included three local catchment reservoirs and water pumped about 50 kilometers (km) from the River Murray via the Murray Bridge-Onkaparinga Pipeline.

There are three local catchment reservoirs in Adelaide's southern water supply system—Myponga, Mount Bold, and Happy Valley (Figure 1), which can hold up to a total of 85 GL of water. Myponga is independent of the other two reservoirs, with water being treated at the Myponga Water Treatment Plant (WTP) before being released into the mains distribution network. However, water from Mount Bold Reservoir must be released downstream and diverted at Clarendon Weir via the Horndale Flume to Happy Valley Reservoir before being treated at Happy Valley WTP and released into mains distribution (Figure 1). Happy Valley Reservoir also receives water from Clarendon Weir Catchment (Figure 1), which is similarly transferred via the Horndale Flume. For a more thorough description of the reservoir properties and operations see *Paton et al*. [2013].

Water from the River Murray is transferred to the southern system via the 48 km long Murray Bridge-Onkaparinga (MBO) Pipeline (Figure 1). It is released upstream of Mount Bold Reservoir (Figure 1), where it can be stored before treatment and distribution. As explained in *Paton et al*. [2013], supply from the River

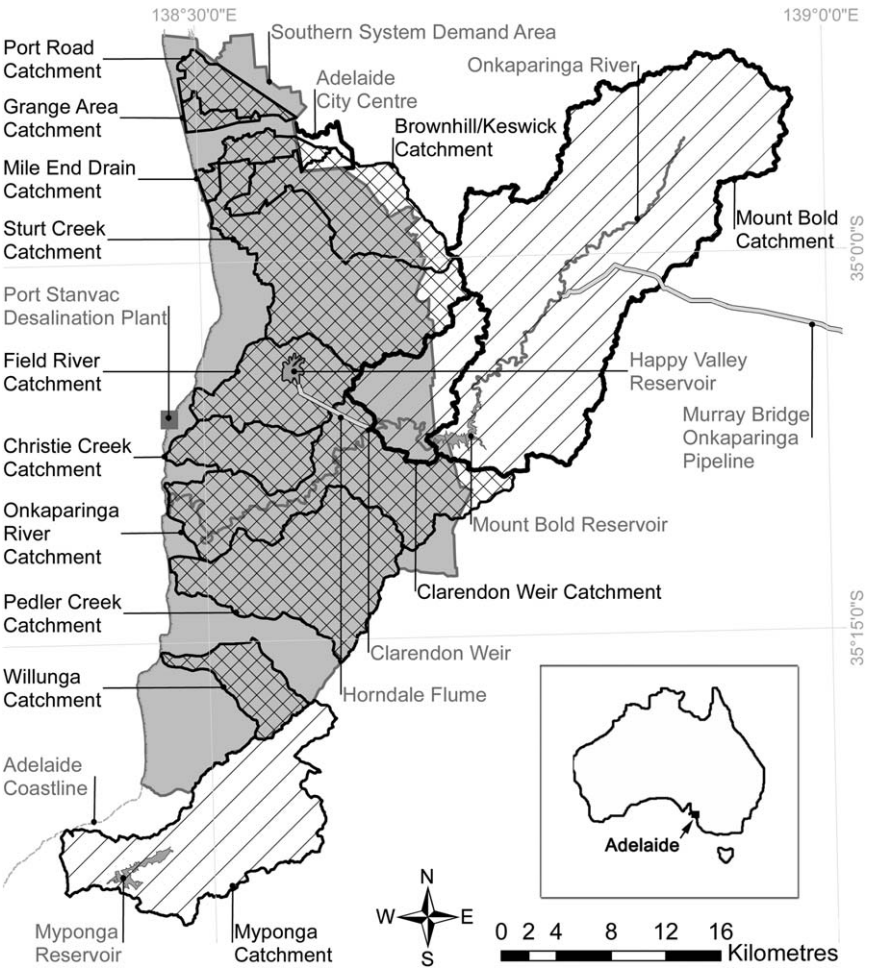

Figure 1. Map of the existing Adelaide southern water supply system, showing reservoirs, reservoir catchments, major rivers, pipelines, and an indicative southern system demand area (illustrated by gray shading). The Port Stanvac desalination plant and the 10 southern water supply system storm water harvesting scheme catchments are also shown. Inset is a map of Australia highlighting the location of Adelaide.

Murray for Adelaide is capped at 650 GL over 5 years under the terms of SA Water's license. While a license does not always guarantee supply, Adelaide's River Murray license has previously always been met, with up to 90% of Adelaide's demand being catered for by the River Murray in dry years [*Government of South Australia*, 2009].

However, to respond to the uncertainties of climate change in the future and an increasing demand due to population growth, supply augmentation for the current Adelaide southern water supply system is necessary to avoid demand shortfall [*Paton et al.*, 2013]. *Maier et al.* [2013] illustrated that a diversification of water supply sources could help the system to meet future demand shortfall through an assessment of five feasible sources for water supply, which comprised the two current supply sources and three potential supply sources. The current sources included pumping from the River Murray via the MBO Pipeline (Figure 1) and local catchment reservoirs (Figure 1). Potential supply sources included a reverse osmosis (RO) desalination plant at Port Stanvac (Figure 1), storm water harvesting schemes that collect water from 10 catchments extending from Port Road catchment in the north to Willunga catchment in the south (Figure 1), and household rainwater tanks.

This paper extends the current understanding of future options for Adelaide's current southern water supply system by using optimization, specifically a multiobjective evolutionary optimization approach, to search a greater number of potential feasible alternatives (including supply operations, as well as increased supply augmentation options), rather than simply analyzing a limited number of discrete options. Demand-

Table 1. Values for Options of Supply Source Augmentation and Supply System Operation Defined for the Case Study

Option	Values for Option
Desalination plant capacity (ML/d)	0, 100, 150, 200, 250, 300, 350, 400, 450, 500
Storm water schemes	Brownhill-Keswick, Sturt River, Field River and Pedler Creek
Rainwater tank size (m^3)	0, 1, 2, 3, 4, 5, 6, 7, 10, 15, 22.5, 27
Rainwater tank roof connectivity (%)	50, 60, 70, 80, 90
Rainwater tank end use	Garden, toilet, laundry cold water, hot water
Supply priority	1, 2, 3, . . ., 7
Supply weight	1, 2, 3, . . ., 10
Mount bold level to trigger River Murray pumping (monthly values, %)	0, 5, 10, . . ., 100

side management options are not examined, as they are outside the scope of this paper. However, as the consideration of water demand reduction strategies can have significant urban water system-wide benefits (in terms of the environment and economic cost) [*Sahely and Kennedy*, 2007], they should be included in future studies. A 40 year planning horizon from 2010 to 2050 was used to assess the alternatives.

4. Methods

4.1. Objectives and Constraints

The selected objectives for the case study include: (1) to minimize system vulnerability; (2) to minimize economic cost; and (3) to minimize GHG emissions. Constraints on system reliability and duration of failure were also applied. Details of how the objectives and constraints were calculated are given in sections 4.4 and 4.5. It should be noted that while the objectives and constraints were kept constant in this study, the benefit of using an adaptive decision-making framework that continually updates the objectives and constraints and enables the GHG emissions objective to be readily assimilated into existing trade-off studies [*Kasprzyk et al*., 2012] could be explored in future studies.

4.2. Water Supply Alternatives

The water supply alternatives comprised both supply source selection and supply system operation. For the supply sources, options included the existing River Murray supply and the three local catchment reservoirs (see section 3), as well as the three potential sources of a desalination plant, storm water harvesting schemes, and household rainwater tanks.

The capacity of the Port Stanvac desalination plant can range between 100 and 500 megalitres per day (ML/d) in 50 ML/d increments (Table 1). These capacities were nominated as they provided a good range of feasible sizes for desalination plants based on current and planned expansion capacities of desalination plants in Australia. However, these capacities were halved for the case study, because the southern system accounts for approximately half of Adelaide's demand. The option of not including a desalination plant was also considered (Table 1).

For storm water, there were four schemes for the southern system that could be selected, namely Brownhill-Keswick, Sturt River, Field River, and Pedler Creek (Table 1). As explained by *Beh et al*. [2014], these schemes represent a total of 10 storm water catchments that predominantly fall in the indicative southern system demand area (Figure 1).

Rainwater tanks could be selected as a supply source, based on a Government policy introduced in 2006 requiring most new homes and home extensions in South Australia to have rainwater tanks installed [*Government of South Australia*, 2009]. The rainwater tanks could take one of 11 sizes, ranging from 1 m^3 up to 27 m^3 (Table 1), as these are feasible sizes when taking the physical size constraints of residential backyards into account. In addition, the fraction of roof connected to the tank could range from 50% up to 90% (Table 1).

When rainwater tanks and harvested storm water schemes were both selected as supply options, the roof connectivity for storm water harvesting was reduced because less roof runoff was assumed to be entering the storm water collection network. Finally, while the rainwater tank was always assumed to be connected to the garden, it could also be connected to one or more of three indoor end uses, namely the toilet, laundry cold water, and hot water (Table 1).

In addition to decisions regarding the size and properties of supply sources, alternatives were also a function of different operating rules of the system. These included determining: (1) which sources would have

Table 2. Demand Type and Water Source for the Five Demand Categories Defined for the Adelaide Southern System Case Study

Category	Demand Type	Water Sources
Type I	Residential—potable	River Murray, local catchment reservoirs, desalination plant
Type II	Residential (garden) nonpotable, climate-dependent	Rainwater, River Murray, local catchment reservoirs, desalination plant
Type III	Residential (toilet)—nonpotable, climate-independent	Rainwater, River Murray, local catchment reservoirs, desalination plant
Type IV	Nonresidential—potable	River Murray, local catchment reservoirs, desalination plant
Type V	Nonresidential—nonpotable	Storm water, River Murray, local catchment reservoirs, desalination plant

priority of supply, if water was available from more than one source; (2) whether more water should be drawn from one source than another if sources had equal priority; and (3) what level Mount Bold Reservoir should reach to trigger pumping of water from the River Murray. For priority of supply, options ranged from 1 to 7 (Table 1), with one being the highest priority and seven being the lowest. For supply weights, options ranged from 1 to 10 (Table 1), with weights being considered relative to each other, so that a source of weighting five would supply five times the amount of water of a source of weighting one (provided the sources had equal priority). For the Mount Bold Reservoir target level (to trigger pumping from the River Murray), each month of the year was assigned a value, ranging from 0% to 100% in 5% increments (Table 1). Given the number of decision variables, the decision space for the optimization problem was 3.26×10^{33}, clearly justifying the need to use MOEAs to efficiently search the space and produce an approximation of the Pareto Front.

4.3. Simulation Model

The water resources model WaterCress (www.waterselect.com.au/watercress/watercress.html) was selected to evaluate alternatives because the model can (1) cater for the alternative water sources and supply operations of the case study (see section 4.2), (2) easily incorporate multiple scenarios (see section 4.7), and (3) be easily linked with an optimization module through the use of text input and output files. It is also freely available, locally supported in Adelaide, and has been previously applied to this case study [*Beh et al*., 2014; *Maier et al*., 2013; *Paton et al*., 2013, 2014]. These publications provide further details of the model, its benefits, and its suitability for the case study.

The WaterCress representation of Adelaide's southern water supply system consisted of two major components—demand and supply. Demand was a function of both population and per capita consumption. The population in 2050 was assumed to be approximately 775,000 people, about half of Adelaide's 2050 population based on the median population projection (derived from 72 projections) [*Australian Bureau of Statistics*, 2008]. For the optimization process, per capita consumption was assumed to remain constant over the planning horizon at 494 liters per capita per day (Lcd) [*Paton et al*., 2013]. This is a conservative approach to demand projection; however, options considering demand reduction through water savings were investigated postoptimization (see section 4.7). In the WaterCress model, per capita consumption was split into five categories (Types I–V) to account for residential and nonresidential, potable and nonpotable, and climate-dependent and climate-independent demands (Table 2). These were important delineations to make in terms of allocating water sources to appropriate end use categories (Table 2). First, rainwater was only used for residential use, second, rainwater, and harvested storm water were both considered nonpotable, and third, garden demand varied considerably depending on the season [see *Paton et al*., 2013], so this variability needed to be modeled.

In terms of supply, sources could be considered as climate-independent or climate-dependent. The River Murray and desalination plant were both classified as climate-independent sources, which is intuitive for the desalination plant but not so for the River Murray. However, in the past, River Murray supply for Adelaide has depended on licenses, rather than climate, and this supply is guaranteed [*Paton et al*., 2013]. In addition to the Mount Bold level to trigger River Murray pumping, River Murray supply was also constrained to 447 ML/d (the pumping capacity of the MBO Pipeline), and 325 GL over 5 years. This second constraint represented half of the 5 year rolling license (see section 3) and was a necessary simplification because WaterCress could not incorporate a rolling license. The local catchment reservoirs, storm water harvesting schemes, and household rainwater tanks were considered to be climate-dependent sources.

Table 3. Economic Cost Summary for Different Water Supply Sources

Supply Source	Capital Costs	Operational Costs
Local catchment reservoirs	n/a	Power and chemical of treating water at the water treatment plants (WTPs) Labor to run the WTPs Mechanical asset replacement Upgrading infrastructure
River Murray	n/a	Treatment at Happy Valley WTP (see above) Electricity for pumping for MBO Pipeline
Desalination	Desalination plant Materials and construction for the transfer pipeline pipe and fittings Pumps and pump station building for transfer pipeline	Electricity Labor Chemicals Membrane and plant replacement Electricity for pumping, and pump replacement, for transfer pipeline
Storm water	Storm water wetland material and construction Aquifer storage recovery material and construction Water distribution network material and construction	Labor Replacement capital Maintenance Electricity for pumping UV treatment Monitoring fees
Rainwater	Tank Delivery and installation Dolomite base Pump (and for indoor use a mains switch) Plumbing	Electricity for pumping Tank maintenance Pump and tank replacement

Consequently, runoff from their catchments (either pervious, impervious or both in the case of storm water), were modeled as a function of rainfall and evaporation, which were sourced from eight representative climate data sites across the indicative demand area and local reservoir catchments (Figure 1). Details on the rainfall-runoff models and the rainfall and evaporation data for this case study can be found in *Paton et al*. [2013, 2014] and *Beh et al*. [2014].

The impact of climate change on local catchment reservoirs, storm water harvesting schemes, and household rainwater tanks was projected by first considering outputs from different world development pathways, represented by SRES scenarios, and different global circulation models (GCMs). For the optimization process, the A1B emissions scenario was used in combination with the CCSM3 GCM. These selections proved to return middle of the range estimates for water supply security when compared with a selection of SRES scenarios and GCMs for a number of different water supply configurations. Alternative SRES scenarios and GCMs were considered postoptimization (see section 4.7). The constant scaling or delta-change approach was then applied to obtain local rainfall and evaporation responses to these climate change projections, as this has been used for this case study previously [*Paton et al*., 2013, 2014].

One thousand 30 year stochastic rainfall time series were generated, ensuring the impact of natural rainfall variability was considered, as this number of replicates guaranteed that the important statistical characteristics of the historical data sets were preserved in the generated data sets [see *Paton et al*., 2013, for more detail]. However, due to computational constraints, only 10 stochastic time series were selected for the optimization process, with the full 1000 stochastic time series subsequently applied in the postoptimization robustness assessment (see section 4.7). The 10 time series were selected to be representative of the 1000 series for a range of different water supply system configurations with different combinations of sources. This was achieved by minimizing the difference between the average maximum annual vulnerabilities obtained using the 10 selected time series and the 1000 time series with the aid of a genetic algorithm.

Finally, the supply priorities and weights were applied (decision variables in the optimization process), to integrate the supply sources in the WaterCress model. However, given the limited capacity of rainwater tanks to store water, if rainwater was available, it was always used as a first priority for its allocated household uses.

4.4. Objective Function Evaluation

Synopses of how vulnerability and economic cost were evaluated for the case study are provided below. More extensive detail is provided for the GHG emissions evaluation due to the significance of incorporating the reduction of GHG emissions as an objective in this paper.

4.4.1. Vulnerability

The vulnerability objective was represented by the maximum annual vulnerability as a percentage of demand averaged over the 10 stochastic time series as follows:

$$M.Vul = \frac{\sum_{t=1}^{T} \max\left(\left\{\frac{V_{at}}{D}\right\}\right)}{T} * 100 \quad (1)$$

where M.Vul was the average maximum annual vulnerability given as a percentage; V_{at} was the volume by which demand exceeded supply (given a failure occurred) for year a of the stochastic time series (a = 1–30) and time series t (t = 1–10); D was the average annual demand; and T was the number of time series evaluated (T = 10).

4.4.2. Economic Cost

Economic costs for existing supply sources (River Murray and local catchment reservoirs) were purely a function of operational costs over the 40 year planning horizon, as their capital costs were considered sunk costs. However, economic costs for new supply sources were a function of both the capital costs incurred in 2010 and operational costs over the planning horizon. Consequently, the 2010 present value total system cost was calculated as

$$\text{2010 PV Total System Cost} = \text{2010 PV OC}_{[RM+Res+Des+SW+RW]} + \text{CC}_{[Des+SW+RW]} \quad (2)$$

where 2010 PV $OC_{[RM+Res+Des+SW+RW]}$ was the sum of the 2010 PV operational costs for the five supply sources and $CC_{[Res+SW+RW]}$ was the sum of the capital costs for desalination, storm water, and rainwater. Due to the extensive economic cost data for supply sources, a summary of economic costs for each supply source is included in Table 3, while a full derivation is provided as supporting information. An indicative cost of 12 cents per kilowatt hour (c/kWh) was assumed as the purchase price for electricity, which is slightly higher than SA Water's average electricity purchase price of approximately 10 c/kWh (see SA Water's 2010 annual report at www.sawater.com.au), so as to account for potential electricity price increases in South Australia over the planning horizon. To convert future operational costs to their 2010 present value, a discount rate of 4% was used for the first 5 years, from 2015 to 2035 (inclusive) the discount rate was reduced to 3%, while this was reduced further to 2% from 1 May 2035 to the end of the planning horizon [*Weitzman*, 2001]. Application of a declining discount rate (DDR) is supported by *Rambaud and Torrecillas* [2005] because of (1) uncertainty about the future, (2) future fairness, and (3) observed individual choice.

4.4.3. Greenhouse Gas Emissions

In a similar way to economic costs, only operational GHG emissions were attributed to existing supply sources, while for new potential supply sources, both operational GHG emissions and capital (embodied) GHG emissions were included. Specifically, total system GHG emissions were calculated as

$$\text{Total System GHG Emissions} = \text{OGHG}_{[RM+Res+Des+SW+RW]} + \text{CGHG}_{[Des+SW+RW]} \quad (3)$$

where $OGHG_{[RM+Res+Des+SW+RW]}$ was the sum of the operational GHG emissions for the five supply sources and $CGHG_{[Res+SW+RW]}$ was the sum of the capital GHG emissions for desalination, storm water, and rainwater. Due to the extensive GHG emissions data for supply sources, a summary of GHG emissions for each supply source is included below, while further detail is provided as supporting information. No discount rate was used for GHG emissions; however, a sensitivity analysis on different discount rates should be investigated in future work. The GHG emissions factor for electricity was assumed to be 0.73 kilograms of carbon dioxide equivalents per kilowatt hour ($kgCO_2^{e-}$/kWh), which is the latest full fuel cycle emissions factor (FFCEF) estimate for purchased electricity by South Australian end users [*Department of Industry, Innovation, Climate Change, Science, Research, and Tertiary Education*, 2013]. South Australia's generated electricity is sourced predominantly from natural gas (52%), wind (27%), coal (17%), and solar (4%) [*Australian Energy Market Operator*, 2014]. Its FFCEF for purchased electricity is thus lower than the Australia-wide average of

1.00 $kgCO_2^{e-}$/kWh, reflecting South Australia's greater uptake of renewable fuels and lower reliance on coal compared to states such as Victoria and New South Wales (FFCEFs of 1.35 and 1.05 $kgCO_2^{e-}$/kWh, respectively) [*Department of Industry, Innovation, Climate Change, Science, Research, and Tertiary Education*, 2013]. However, it is comparatively high compared to Tasmania's FFCEF of 0.22 $kgCO_2^{e-}$/kWh [*Department of Industry, Innovation, Climate Change, Science, Research, and Tertiary Education*, 2013], which relies heavily on hydropower. From an international perspective, Australia's FFCEF for purchased electricity is relatively high due to its energy sector being one of the most CO_2-intensive in the world, along with other coal-dependent countries such as South Africa, India, and Indonesia [*Foster and Bedrosyan*, 2014]. Natural-gas dependent countries, such as Mexico and Egypt, have lower emissions factors, while even lower emissions factors exist for hydropower-dependent countries, such as Canada and Brazil [*Foster and Bedrosyan*, 2014]. For example, in 2009, Canada's electricity generation emissions factor, including transmission losses and associated emissions, was 0.20 $kgCO_2^{e-}$/kWh [*Canadian Government*, 2011].

4.4.3.1. Local Catchment Reservoirs and River Murray

For local catchment reservoirs, operational GHG emissions associated with the energy required for treatment at the WTPs and those associated with chemical use were accounted for. Operational GHG emissions of River Murray supply included GHG emissions of treating the water at Happy Valley WTP and GHG emissions due to pumping. GHG emissions due to pumping were derived from first principles, using the Darcy-Weisbach head loss equation and the pump power equation (see section 2 of supporting information on economic costs). The pump power was then converted to energy requirements, based on 24 h operation, before being transferred to GHG emissions.

4.4.3.2. Desalination

Capital GHG emissions for the desalination plant were attributed to the materials, electricity, and diesel used to construct the main plant and onsite power facilities, which account for just less than 1% of operational GHG emissions over a 20 year plant lifetime. Using this relationship and the derived operational GHG emissions, the capital GHG emissions were estimated for each desalination plant capacity. For the desalination plant transfer pipeline, capital GHG emissions associated with materials for the mild steel cement lined (MSCL) pipeline and construction of the pipeline were accounted for. GHG emissions associated with the materials for the pumps were considered insignificant based on the GHG emissions inventory of the similarly sized Murrumbidgee to Googong pipeline [*ACTEW Corporation*, 2009].

Operational GHG emissions included electricity required for treatment, chemicals, and membrane and plant replacement. The GHG emissions associated with membrane replacement were applied every 5 years and were independent of the amount of water produced by the plant. Furthermore, the GHG emissions associated with plant replacement were accounted for once in 2030 and were estimated to be the same as the initial capital GHG emissions. However, GHG emissions associated with power and chemicals depended on the amount of water supplied by the desalination plant. The operating GHG emissions for the transfer pipeline were attributed to the electricity required to power the transfer of water. The power required to pump the water was estimated using first principles (see section 2 of supporting information on economic costs). GHG emissions associated with pump replacement were excluded, as they were negligible compared with GHG emissions associated with pumping.

4.4.3.3. Rainwater Tanks

Capital GHG emissions were attributed to the rainwater tank, pump, pipes, fixtures, and installation. However, the transport of the rainwater tank system to site was not accounted for, as this was expected to vary considerably for each house. All rainwater tanks were assumed to be made from high-density polyethylene (HDPE).

Operational GHG emissions for rainwater tanks were attributed to electricity use of the pump and replacement of the tank (25 years) and pumps (10 years). However, no replacement GHG emissions associated with pipes nor fixtures were accounted for, as these were assumed to have a lifetime greater than the planning horizon. Replacement GHG emissions for the tanks and pumps were assumed to be the same as the initial capital GHG emissions.

4.4.3.4. Storm Water Schemes

The capital material and construction GHG emissions for the storm water schemes were attributed to the materials and construction of the wetland, aquifer storage and recovery (ASR) wells, and the distribution

network. The GHG emissions associated with pumps were not considered, given that GHG emissions for pumps of large pipelines were found to be negligible compared to other capital GHG emissions and the operating GHG emissions of pumps. For the wetlands and ASR wells, GHG emissions were attributed to the concrete and steel used in their construction and the excavation of soil required to create the wetlands and wells.

For the distribution network, pipes were assumed to be made from HDPE, have a pressure rating of 600 kilopascal (kPa), an outside diameter of 280 mm, and a wall thickness of 10.8 mm. The length of pipeline required for the distribution of harvested storm water to nonpotable industrial and commercial users was estimated from a number of similar storm water schemes in Adelaide. Specifically, the following equation was derived to estimate pipe length based on the potential yield of the schemes

$$L = 18.108 * Y^{0.5681} \tag{4}$$

where L is the length of pipeline (in km) and Y is the potential yield of the storm water scheme (in GL/yr).

Operational GHG emissions for the storm water harvesting schemes were based on operating GHG emissions, namely those associated with pumping the storm water. The wetlands, wells, and distribution network were assumed to have lifetimes greater than the planning horizon of 40 years considered, so no GHG emissions associated with replacement were attributed to storm water harvesting. GHG emissions for pump replacement were also ignored, as these were assumed to be negligible compared with those associated with the electricity required for pumping.

4.5. Evaluation of Constraints

Constraints were based on the definition of "acceptable performance" representing the extent of water savings that can be expected from temporary water restrictions, which is a function of the "acceptable" frequency, duration, and severity of restrictions [*Chong et al*., 2009a]. As Adelaide has no defined "level of service" objectives in terms of these measures [*Chong et al*., 2009a], "acceptable performance" was based on the "level of service" objectives for Melbourne, Australia, which include reliability $>$95% and duration of failure $<$365 days [*Chong et al*., 2009a].

Reliability was calculated as

$$\mathrm{Re}\,I = \frac{\sum_{t=1}^{T}\left(\frac{S_t}{D_t} * 100\right)}{T} \tag{5}$$

where Rel was the average reliability of the system given as a percentage; S_t was the number of days available supply exceeded demand (success state) for time series t (t = 1–10); D_t was the total number of days evaluated for time series t (D_t = 10,958); and T was the number of time series evaluated (T = 10).

Average maximum duration of failure was calculated as

$$M.D.F. = \frac{\sum_{t=1}^{T} \max\left(\{F_t\}\right)}{T} \tag{6}$$

where M.D.F. was the average maximum duration of failure given in days; F_t was the number of consecutive days that demand exceeded supply given a failure occurred for time series t (t = 1–10); and T was the total number of time series evaluated (T = 10).

4.6. Optimization

The Water System Multiobjective Genetic Algorithm (WSMGA) developed by *Wu et al*. [2010], which is based on the nondominated sorting genetic algorithm II (NSGA-II) [*Deb et al*., 2002], was used as the multiobjective genetic algorithm (MOGA), as it has been shown to perform well in previous studies and caters to discrete decision variables.

In order to calibrate the WSMGA, various values of the population (P) (50–300), number of generations (G) (100–400), probability of crossover (P_c) (0.6–0.9), and probability of mutation (P_m) (0.05–0.2) were trialed. In order to identify the most appropriate combination of these parameters, the hypervolume of the different Pareto Fronts produced whilst varying the parameters was analyzed. The hypervolume was selected for this purpose because it is the most difficult metric to satisfy, given it rigorously captures both convergence and diversity of the Pareto Front [*Reed et al*., 2013]. Specifically, for different combinations of P, P_c, and P_m, the hypervolume was plotted against the number of generations, with the aim of determining which combination of P, G, P_c, and P_m returned the largest hypervolume (and so resulted in a Pareto front with good convergence and diversity) with the least computational effort. The parameters obtained through this process were $P = 150$, $G = 150$, $P_c = 0.9$, and $P_m = 0.1$.

The random initialization of the first generation in WSMGA was repeated 10 times, with the final Pareto Front comprised Pareto optimal points sourced from all 10 runs. A number of runs was necessary to ensure that near-globally optimum solutions were found, because WSMGA is a stochastic algorithm and will thus find different solutions depending on the starting position in the search space [*Keedwell and Khu*, 2006].

4.7. Postoptimization Robustness Assessment

To provide an indication of how robust the solutions were to future uncertainties in demand and impacts of climate change projections [see *Paton et al*., 2013], six solutions from the Pareto front were subjected to multiple future scenarios in a postoptimization robustness assessment.

These solutions were selected because they (a) represented breakpoints in trade-offs between two of the three objectives (Figures 2b–2d); (b) spanned a wide range of values of the objectives, i.e., solutions were across the Pareto surface, rather than only from a small section of the surface (Figure 2a); and (c) had average maximum annual vulnerabilities of less than 27% of demand. This cut-off was employed as it is equivalent to the projected savings under Adelaide's toughest level 5 water restrictions [*Chong et al*., 2009b], and thus the upper limit of this objective to ensure system failure was prevented.

Overall, 252 scenarios comprised six SRES scenarios, seven GCMs (from the set of coordinated climate model experiments comprising the World Climate Research Programme's Coupled Model Intercomparison Project CMIP3), and six demands were included in the robustness assessment. This is consistent with the scenarios applied to this case study by *Paton et al*. [2013]. The six SRES scenarios included B1, B2, A2, A1B, A1T, and A1FI, which were selected to cover the full range of potential future development pathways defined by the Intergovernmental Panel on Climate Change. The GCMs were selected using CSIRO's Climate Futures Framework (CFF) [*Clarke et al*., 2011], in which plausible climates simulated by GCMs are classified into a small set of representative climate futures (RCFs) [*Whetton et al*., 2012]. Consequently, a smaller subset of GCMs can be selected that cover the identified RCFs (in this case study six RCFs were identified), thus reducing computational effort but still maintaining the uncertainty in GCM projections.The seven GCMs selected for this case study using the CFF included CCSM3 (hereinafter CCSM), CGCM3.1(T63) (hereinafter CGCM-h), CSIRO-MK3.5 (hereinafter CSIRO), FGOALS-g1.0 (hereinafter FGOALS), MIROC3.2(hires) (hereinafter MIROC-h), MIROC3.2(medres) (hereinafter MIROC-m), and MRICGCM2.3.2 (hereinafter MRI). The six demand scenario options, labeled Very low, Low, Medium low, Medium high, High, and Very high, represented three population estimates combined with two per capita consumption estimates (Table 4), as detailed in *Paton et al*. [2013].

For each of the six selected solutions, the WaterCress model was run for each of the 252 scenario options in combination with the 1000 stochastic time series. Robustness was then estimated as

$$Rob = S/T \tag{7}$$

where Rob was the robustness, S was the number of scenarios for which the system was considered to exhibit "acceptable performance" and T was the total number of scenarios evaluated ($T = 252{,}000$). As discussed earlier, "Acceptable performance" was defined in terms of a reliability $>95\%$, a maximum duration of failure <365 days, and a maximum vulnerability $\leq 27\%$ of demand.

In addition, the median values for the 1000 stochastic time series for each of the 252 scenarios for the each of the selected solutions for average maximum annual vulnerability, average reliability, average

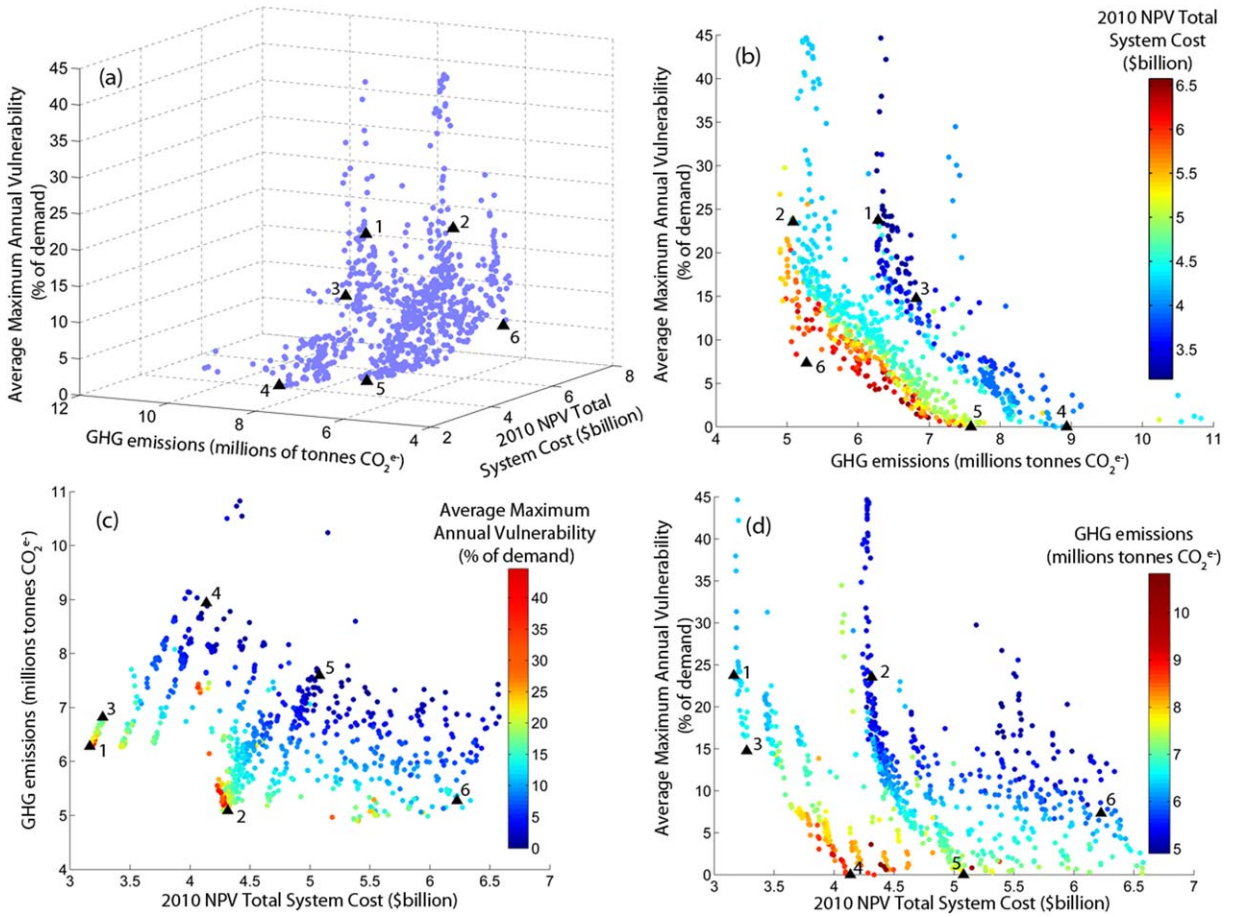

Figure 2. The Pareto front for the case study illustrating trade-offs between (a) all three objectives; (b) average maximum annual vulnerability and GHG emissions; (c) GHG emissions and 2010 NPV total system cost; and (d) average maximum annual vulnerability and 2010 NPV total system cost. The black triangles indicate the six solutions (numbered to correspond with Tables 6 and 7) selected for the postoptimization robustness assessment.

maximum duration of failure, total system cost, and total GHG emissions were calculated so as to assess how the uncertainty sources (GCMs, SRES scenarios, and demands) affected the performance criteria. This was important from a practical management perspective, as if the greatest sources of uncertainty are within the control of the water authority, any effort may be best spent by reducing this uncertainty, thus resulting in a smaller future window of uncertainty and increasing the robustness of solutions. It should be noted that while in this instance median values were selected for comparison, a more conservative approach would be to look at the values for which only 5% or 10% of future scenarios would be more vulnerable, more costly, more GHG emissions intensive, less reliable, and have more consecutive days of failure.

Table 4. Demand Scenario Options

Demand Scenario	Per Capita Consumption	Population Growth
Very low	Reduction	Small
Low	Constant	Small
Medium low	Reduction	Medium
Medium high	Constant	Medium
High	Reduction	Large
Very high	Constant	Large

5. Results and Discussion

The Pareto front illustrating the range of values of the objectives and the trade-offs between objectives for the nondominated solutions is presented in section 5.1. Analysis of the Pareto front, in terms of the similarities in decision variables for solutions comprising the Pareto front, is presented in section 5.1.1, while section 5.1.2 examines how decision variable selection affects the objectives. In

Table 5. Median Unit Costs and GHG Emissions (Includes Both Capital and Operational Costs and GHG Emissions) Derived From the 792 Pareto Optimal Solutions for the Different Supply Sources

Supply Source	Median Unit Cost ($/m^3)	Median Unit GHG Emissions ($kgCO_2^{e-}/m^3$)
Myponga Reservoir local catchment	0.35	0.18
Happy Valley Reservoir local catchment	0.09	0.09
River Murray	0.16	0.82
Desalination plant	2.32	3.78
Household rainwater tanks	2.36	1.89
Brownhill-Keswick storm water harvesting scheme	1.12	0.48
Sturt storm water harvesting scheme	1.39	0.57
Field storm water harvesting scheme	1.42	0.59
Pedler storm water harvesting scheme	1.26	0.54

section 5.2, the postoptimization robustness results are presented, thereby investigating (a) how robust the six solutions are to future uncertainties when assessing the impacts of climate change on water supply (including demand uncertainty) and (b) which uncertainty sources have the greatest impact on the objective values. A summary of the results from a practical management perspective is given in section 5.3.

5.1. Optimization

Four different views of the Pareto front (comprising of 792 nondominated solutions) are presented to fully illustrate the trade-offs between the three objectives (Figures 2a–2d). Because of the large number of nondominated solutions, decision-makers may also benefit from investigating a number of interactive visual analytics, as highlighted by *Kasprzyk et al*. [2009, 2012, 2013]. However, the Pareto fronts do illustrate a number of patterns, the most evident being that trade-offs exist between all three objectives. First, decreases in average maximum annual vulnerability result in increases in costs and/or GHG emissions (Figures 2b and 2d). However, the rate of increase varies. Relatively large vulnerabilities can be reduced to small values with only small increases in costs and/or GHG emissions, while completely removing system failure is much more expensive and/or GHG emissions intensive. For example, in moving from solutions 1 to 3, a reduction in average maximum annual vulnerability of 9% is associated with a relatively small 3% increase in economic cost, whereas a further reduction of 15% in average maximum annual vulnerability to achieve no system failure (e.g., solution 4) comes at a minimum additional 27% increase in economic cost (Figure 2d). Similarly, for GHG emissions, in moving from solutions 2 to 6, average maximum annual vulnerability can be cut from 23.5% to 7.3% with only a 3.5% increase in GHG emissions, whereas a further reduction of 7.3% of average maximum annual vulnerability (e.g., solution 5) means a minimum additional 44.0% increase in GHG emissions (Figure 2b). Furthermore, there is also a trade-off between costs and GHG emissions, whereby an improvement in GHG emissions or cost does not necessarily correlate with an improvement in the other objective (Figure 2c). For example, for solutions 1 and 2, which have very similar average maximum annual vulnerability (Figures 2b and 2d), solution 2 costs $1.15 billion more than solution 1, while solution 1 has greater GHG emissions, specifically 1.19 million tonnes of CO_2^{e-} more than solution 2 (Figure 2c). The objective values also range considerably, with average maximum annual vulnerability varying from 0% to 44.7% of demand, total system cost from $3.17 to $6.58 billion, and GHG emissions from 4.90 to 10.83 million tonnes of CO_2^{e-} (Figure 2).

5.1.1. Decision Variables

A number of trends in the values for the decision variables are apparent when studying the solutions that comprise the Pareto front (Figure 2). First, a desalination plant is always selected, with capacity between 100 and 500 ML/d (representing the full range of options specified for this variable, except for the option of no desalination plant). This seems counterintuitive from purely studying the unit costs and GHG emissions of desalination, as desalination is almost the most expensive source and is the most GHG emissions intensive (Table 5). However, this source is being selected because of the third objective—risk-based performance. That is, even the smallest desalination plant capacity (approximately 36.5 GL/yr) could supply more water than all of the storm water schemes (maximum supply from Pareto solutions of 17 GL/yr) and rainwater (maximum supply from Pareto solutions of 25 GL/yr). Thus, the reliability and duration of failure constraints of the optimization problem may not be met without the desalination plant, resulting in all solutions on the Pareto front containing desalination. The four storm water harvesting schemes are also present in almost every option. This is expected, considering they have both lower unit costs and GHG emissions compared with the two other augmentation options of desalination and rainwater (Table 5). However, as

Table 6. Values for the Capital Decision Variables for the Six Solutions Selected for the Postoptimization Robustness Assessment

Solution Number	Desalination Plant Capacity (ML/d)	Rainwater Tank Size (m^3)	Rainwater Roof Connectivity	Rainwater End Use	Storm Water Schemes
1	150	0	n/a	n/a	All schemes
2	100	3	0.9	Garden, cold laundry, hot water	All schemes
3	150	0	n/a	n/a	All schemes
4	250	0	n/a	n/a	All schemes
5	150	4	0.9	Garden, cold laundry, hot water	All schemes
6	500	5	0.9	Garden, cold laundry, hot water	All schemes

demonstrated by the results, augmentation options in addition to storm water (desalination or desalination plus rainwater) are necessary, as the total potential yield from all of the storm water schemes is insufficient to meet projected future demand.

Rainwater tanks are only present in 70% of the Pareto front solutions, so depending on how important the water authority considers each objective, rainwater tanks may or may not have a place in the future water supply system. Furthermore, when tanks are selected, they are always sized between 2 and 7 m^3, there is a roof connectivity of 0.9 in most cases, and rainwater is usually selected to supply all but the toilet end use (i.e., garden, cold laundry and hot water). It is not surprising that large tank sizes do not feature in the Pareto solutions, because larger tanks do not necessarily supply much more water than smaller tanks in Adelaide's climate, even though they are more expensive and are associated with the emission of more GHGs.

As far as optimal operational decisions are concerned, the desalination plant and Happy Valley Reservoir have the lowest priorities of supply in 84% and 85% of the Pareto solutions, respectively. The relatively high unit costs and GHG emissions for desalination (Table 5) offer a good reason for why desalination has such a low priority. Furthermore, while supply from the Happy Valley Reservoir local catchment has the smallest unit GHG emissions and smallest unit costs, water supplied from Happy Valley Reservoir also contains River Murray supply, which has the second highest unit GHG emissions and thus explains why Happy Valley Reservoir also has a low priority in many solutions. These results suggest that to reduce costs and/or GHG emissions of the system, desalinated and River Murray supply should be used sparingly. There were no distinguishing features in regard to the weights of supply, or the Mount Bold reservoir trigger levels, suggesting that the value these variables take do not have as large an impact on the objective functions as either the capital decisions associated with source augmentation, or the priorities of supply.

5.1.2. Correlations Between Decision Variables and Objectives

There is a 71% positive correlation coefficient between rainwater tank size and economic cost, together with a similar positive correlation coefficient, albeit it slightly less at 60%, between desalination plant capacity and economic cost. This was to be expected, given that larger rainwater tanks and larger desalination plants are more expensive. Supply from local catchment reservoirs, the River Murray, and harvested storm water have much less of an impact on cost, although all correlations are slightly negative. This was to be expected, as increases in rainwater and desalination supply (which are positively correlated with cost) generally mean less water is supplied from the other sources. However, the exception to this is the relationship between supply from desalination and harvested storm water, in which a positive correlation coefficient of 44% exists. This occurs because when rainwater tanks are an option, there is a reduction in the

Table 7. Criteria Values for the Six Solutions Nominated for the Postoptimization Robustness Assessment

Solution Number	2010 NPV Total System Cost ($billion)	Total System GHG Emissions (Millions Tonnes CO_2e^-)	Average Maximum Annual Vulnerability (% of Demand)	Reliability (%)	Average Maximum Duration of Failure (Days)	Robustness (% of Scenarios Exhibiting Acceptable Performance)
1	3.16	6.28	23.7	95.1	92.9	64.8
2	4.31	5.09	23.5	95.5	116.6	43.9
3	3.27	6.82	14.7	95.1	73.6	63.9
4	4.14	8.94	0.0	100.0	0	78.7
5	5.08	7.59	0.0	100.0	0	80.6
6	6.23	5.27	7.3	97.3	28.5	78.7

impervious catchment of harvested storm water. Consequently, harvested storm water yield decreases when rainwater tanks are implemented, which is matched by a decrease in supply from the desalination plant, as less water is required to be supplied by this source (supply from rainwater tanks and the desalination plant have a negative correlation coefficient of 84%).

Rainwater tank selection also influences GHG emissions considerably. For example, all solutions without rainwater tanks have GHG emissions of more than 6.26 million tonnes CO_2^{e-}, in combination with a negative 52% correlation coefficient between rainwater tank size and GHG emissions. In fact, only 2 out of 69 Pareto solutions with GHG emissions of more than 8 million tonnes CO_2^{e-} include a rainwater tank. This infers that rainwater tanks could be useful adaptation measures that also maintain relatively low GHG emissions for the system. While desalination plant capacity only exhibits a 12% correlation coefficient with GHG emissions, desalination plant supply has a 91% positive correlation coefficient with GHG emissions. This implies that: (a) the desalination plant should be used sparingly to minimize GHG emissions (supporting the conclusion in section 5.1.1); and (b) the operational GHG emissions of desalination are more significant than the capital GHG emissions, which is consistent with estimations of capital versus operational energy for desalination plants. Furthermore, there is a negative 56% correlation coefficient between River Murray supply and GHG emissions, inferring that use of the River Murray may also help to reduce GHG emissions of the system. This is as expected, because there is also a negative 45% correlation coefficient between River Murray supply and desalination supply, so when more water is sourced from the River Murray, generally less is sourced from the desalination plant, resulting in fewer GHG emissions. While supply from the local catchment reservoirs also exhibited a similar negative correlation with GHG emissions, there was a slight (25%) positive correlation coefficient between GHG emissions and supply from the harvested storm water schemes. This was expected though, because there is a positive correlation between supply from harvested storm water schemes and the desalination plant, as explained in the preceding paragraph.

5.2. Postoptimization Robustness Assessment

The capital decision variables for the six solutions selected for the postoptimization robustness assessment are summarized in Table 6, while Table 7 summarizes the criteria values derived from the optimization process, as well as the robustness of each solution. While the six solutions all contained the four storm water schemes, the desalination plant capacity ranged from 100 to 500 ML/d and rainwater tanks from 3 to 5 m^3, if they were selected (Table 6). For the three scenarios with rainwater tanks, each had a constant roof connectivity of 0.9, with rainwater used for the garden, cold laundry, and hot water (Table 6). While solutions 1 and 3 have the same capital decision variables (Table 6), the average maximum annual vulnerability is somewhat less for solution 3 (Table 7). Moreover, solution 6, which has a larger supply infrastructure portfolio than solutions 4 and 5 (Table 6), exhibits a few short, small system failures, while solutions 4 and 5 can still provide the required demand (Table 7). These occurrences illustrate that system operation can influence the objectives, even if they may not affect them to the same extent as capital decisions.

The most robust solution to the climate change impact assessment uncertainties is solution 5 at 80.6%, although this is only slightly better than solutions 4 and 6, which share a robustness of 78.7% (Table 7). This is to be expected, given that solutions 4 and 5 exhibit no failures from the optimization runs and thus have the best risk-based performance, while solution 6 in the optimization run only exhibits infrequent failures that are short and of a small magnitude (Table 7). The least robust solution is solution 2, while solutions 1 and 3 (which share the same initial capital decision variables) perform acceptably for about two-thirds of future scenarios (Table 7). So, although solutions 1 and 2 both exhibit very similar average maximum annual vulnerability in the optimization process (Table 7), solution 1 is considerably more robust than solution 2, inferring it has a better overall risk-based performance than solution 1. This makes sense, as the 3 m^3 rainwater tank cannot supply as much water as an additional 50 ML/d capacity for the desalination plant (Table 6).

A summary of the variation in performance criteria due to the different sources of uncertainty for the six solutions (Table 6) is provided below, including boxplots of the variation in average maximum annual vulnerabilities (Figure 3), while boxplots for the other performance criteria are included in the supporting information. Each boxplot has three sections—the top section compares across GCMs, the middle section across SRES scenarios, and the bottom section across demands (e.g., Figure 3). Within each section, the six or seven different scenario options are illustrated, and within each of these, there are six columns that

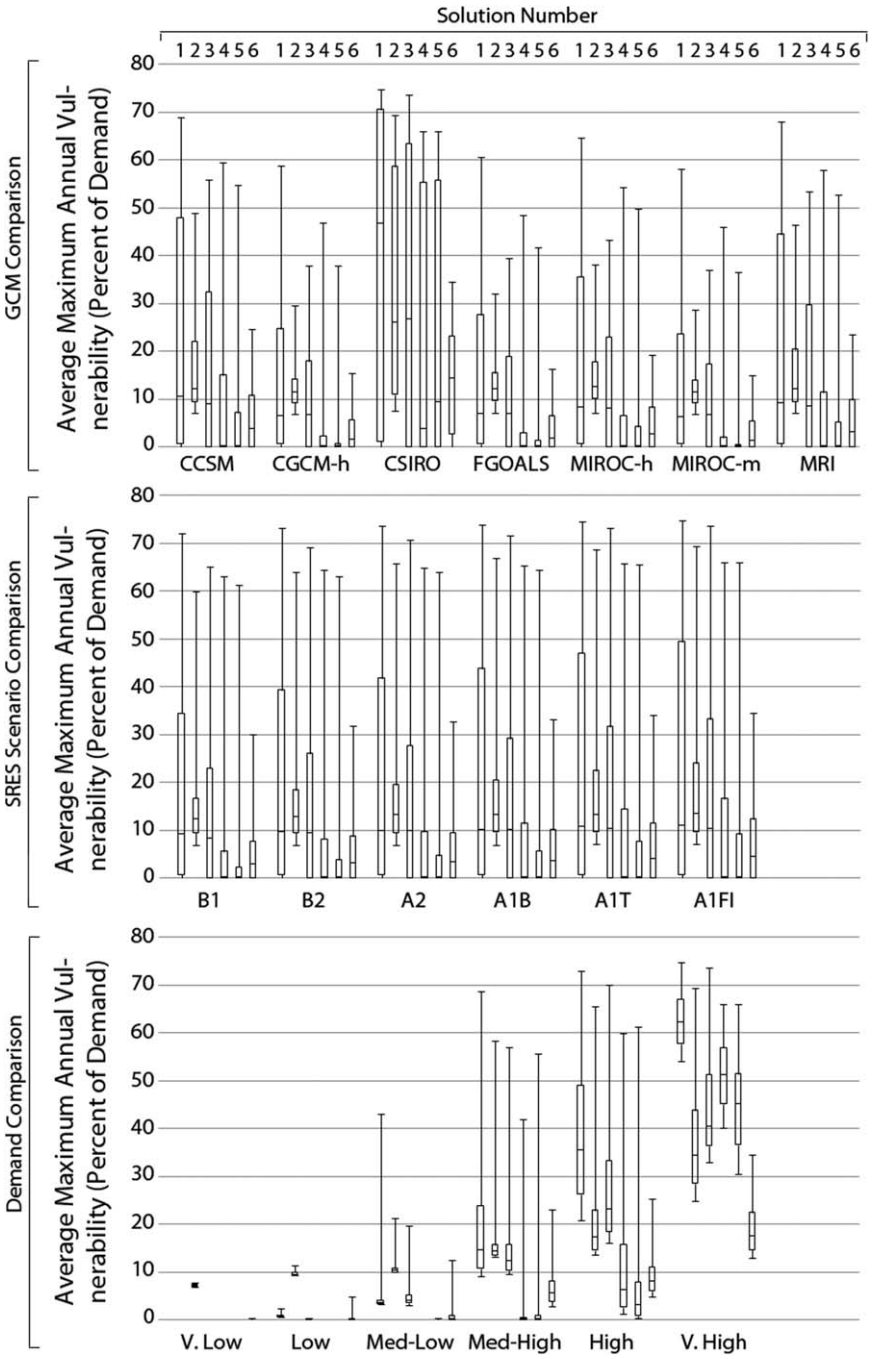

Figure 3. Boxplot of average maximum annual vulnerability comparing the (top section) different GCMs, (middle section) different SRES scenarios, and (bottom section) different demands.

represent each of the six solutions considered in the postoptimization robustness assessment (consecutively from solution 1 in the furthest left column through to solution 6 in the furthest right column). For example, in the top section of each boxplot, for each GCM and each alternative, the columns represent 36 points (one for each of the six SRES scenarios combined with the six demands).

System cost is most insensitive to future uncertainty; however, the costs of solutions with rainwater tanks are more sensitive to changes in population than solutions without rainwater tanks (see supporting information). This is expected, considering the large impact rainwater tanks have on economic cost and given that for larger populations, there are more houses and thus more rainwater tanks. GHG emissions similarly

increase for scenarios with bigger populations, as well as bigger per capita consumptions (see supporting information). This is because larger demands require more water to be supplied, which is likely to increase the supply from desalination plants, which has a major impact on GHG emissions. As illustrated by the increase in average maximum annual vulnerability (Figure 3), larger demands also decrease the risk-based performance of the system (see supporting information). In fact, of the uncertainty sources, demand has the greatest impact on the performance criteria, followed by GCMs and SRES scenarios, as illustrated by a greater variation in the performance criteria when comparing across the different demands, than exists when comparing across the GCMs and SRES scenarios (Figure 3 and supporting information).

5.3. Practical Management Implications

The results from this case study have a number of practical management implications. First, considerable trade-offs exist between (1) cost and risk-based performance and (2) GHG emissions and risk-based performance, which is to be expected, as a system that has enhanced water security, will generally cost more and/or emit more GHG emissions. However, results also illustrated that while large system failures may be reduced to smaller ones relatively cheaply and/or without many additional GHG emissions, to reduce average maximum annual vulnerability to zero will be relatively expensive and/or produce many more GHG emissions. Consequently, it may be better to operate the system with the need for some water restrictions in order to avoid system shortfalls.

A trade-off also exists between economic cost and GHG emissions. The main drivers of this trade-off are the presence of rainwater tanks and the supply of water from the desalination plant. That is, rainwater tanks are an expensive adaptation source and desalination is a GHG emissions-intensive source. Consequently, for a water authority aiming to minimize GHG emissions (as would be the aim in attempting to mitigate the impacts of climate change), water supply from the desalination plant should be kept to a minimum. Therefore, while a desalination plant may be a good adaptation measure to climate change due to its climate independence, other water sources, such as rainwater tanks and storm water harvesting schemes, may be better mitigation measures. This illustrates the importance of accounting for GHG emissions in urban water supply system planning, as if simply cost and risk-based performance were considered as objectives, solutions would favor adaptation responses, rather than mitigation responses.

However, in the future water supply system plan, a desalination plant of some capacity should be included, as it is required to maintain "acceptable" risk-based performance of the system. Similarly, storm water schemes should be included. However, as discussed above, from a mitigation perspective (with the aim of minimizing GHG emissions), the desalination plant should be used sparingly and rainwater tanks between 2 and 7 m^3 should be included, connected to as much of the roof area as possible and supplying garden, cold water laundry, and hot water use. Furthermore, to cope with future uncertainty, some consideration should be given to the outcome of the scenario-based sensitivity analysis. Solutions with a combination of a desalination plant of $\geq$150 ML/d and rainwater tanks of 4 or 5 m^3, or a desalination plant $\geq$250 ML/d, are more robust than solutions with a 100 ML/d desalination plant and 3 m^3 rainwater tanks, or a desalination plant $\leq$150 ML/d. Consequently, planning a system with a desalination plant $\geq$150 ML/d in combination with rainwater tanks will help the system cope with future uncertainty. Furthermore, while uncertainties in GCMs and SRES scenarios both influence the risk-based performance of the system, the greatest impact is due to demand uncertainty. This is comforting to water managers, as per capita consumption is, to an extent, within their control, unlike GCMs and SRES scenarios, for which they cannot reduce the uncertainty. Consequently, reducing per capita consumption, and thus the uncertainty in demand projections, would be a good focus for the water authority, as it would reduce the uncertainty in projecting risk-based performance, and thus improve the robustness of solutions.

6. Summary and Conclusions

While the adaptation of urban water supply systems to climate change has been given due consideration in the literature [see for example, *Wilby and Dessai*, 2010], there still exists a lack of understanding of mitigation responses in planning urban water supply systems. In fact, energy use and GHG emissions are on the rise in the water sector, with some water resource adaptation measures (e.g., desalination plants) having greater energy intensities than traditional sources. However, mitigation responses to climate change require the reduction of GHG emissions. Therefore, due to this contradiction, there is a need to account for both

adaptation and mitigation responses to climate change in urban water supply planning. Furthermore, the mitigation of climate change by minimizing GHG emissions will inevitably conflict with other water supply system objectives, such as maximizing risk-based performance. Thus, balancing and negotiating multiple objectives are a necessary focus. MOEAs are particularly useful tools for addressing such a problem, because they can evolve an approximation to the entire trade-off (Pareto) fronts of multiple objectives in a single run [*Reed et al*., 2003].

In order to address this issue, a MOEA approach was used to optimize future water supply options for the southern portion of Adelaide's water supply system in terms of costs, GHG emissions, and water supply security. The results showed that GHG emissions produced by urban water supply systems can vary considerably (between 4.90 and 10.83 million tonnes of CO_2^{e-} for Pareto solutions of Adelaide's southern water supply system). In addition, there is a trade-off between GHG emissions and risk-based performance and, variation in the rate of increase in GHG emissions with increase in risk-based performance. To reduce relatively large system failures to relatively small ones does not necessarily increase GHG emissions (and/or economic cost) by much; although to completely remove system failure may greatly increase GHG emissions (and/or economic cost). There is also a trade-off between GHG emissions and cost, with solutions resulting in lower GHG emissions potentially costing more. The results also indicated that Pareto solutions comprising a large supply from the desalination plant result in greater GHG emissions, while low GHG emissions solutions favor household rainwater tanks. Thus, while a desalination plant may be a good adaptation measure to climate change due to its climate independence, other water sources, such as rainwater tanks and storm water harvesting schemes, which emit fewer GHG emissions, may be better mitigation measures. Including GHG emissions as an objective in an optimization framework for urban water supply system planning under climate change is thus imperative to ensure that both adaptation and mitigation measures to climate change are considered.

All Pareto solutions generally comprise storm water schemes and a desalination plant to ensure "acceptable performance," and a little over two-thirds of solutions incorporate rainwater tanks between 2 and 7 m^3, inclusive. Rainwater tanks are usually always connected to 90% of the roof, and supply the garden, laundry cold water, and hot water end uses, but not toilets. The operational variables have less of an impact on the objectives compared with the capital investment decisions, although results indicate that operation of the system still influences the objective values, so system operation is still important to consider. Finally, the postoptimization robustness assessment highlighted that three of the six solutions analyzed satisfy the security of supply criteria for about 80% of future scenarios. These three relatively robust solutions include either: (1) a combination of a desalination plant of $\geq$150 ML/d and rainwater tanks of 4 or 5 m^3; or (2) a desalination plant $\geq$250 ML/d. Furthermore, demand uncertainty has the greatest impact on the objectives, so effort directed toward reducing per capita consumption (and thus demand) may be warranted to increase the robustness of solutions to future uncertainties of climate change.

There are a number of limitations of this study that could be addressed in future work. First, a number of assumptions were made regarding values used in modeling the water supply system (e.g., in the catchment rainfall-runoff models) and in estimating costs and GHG emissions (e.g., the price and emissions factor for electricity and the discount rate). These may affect the results of the case study, thus a sensitivity analysis on these factors should be conducted as part of future work. Second, a limitation of the approach is the use of a robustness measure postoptimization. By only considering robustness postoptimization, system operation could not be optimized for each of the scenarios, even though in reality once the initial capital decisions are made, the operation of the system enables some flexibility to react to the actual scenario that eventuates. Further work could therefore focus on reoptimizing just the operational rules for fixed infrastructure options for different future scenarios, to investigate how much adaptive capacity selected infrastructure options have. Third, demand management options (e.g., water rebates for water efficient appliances) were not included as decision variables, as there were insufficient economic cost and GHG emissions data to do so. Therefore, future work should focus on collecting these data, or developing approaches to estimate the costs and GHG emissions for such options, so they can be included as decision variables in the optimization process. Finally, due to the large integrated nature of the approach and the effort required to demonstrate it for a city's water supply system, the approach could only be illustrated for one case study. While the practical management implications drawn from this case study are useful and may be applicable to other urban water supply systems, the application of the approach to a number of cities around the

world would enable more generic conclusions to be drawn about the role of GHG emissions in urban water supply systems and the trade-offs that may exist between adaptation and mitigation responses to climate change.

Acknowledgments
Thanks are due to the University of Adelaide and eWater CRC for their financial support of this research. The assistance of David Cresswell and Richard Clark for their ongoing support of WaterCress and Sri Srikanthan for his help with SCL is gratefully acknowledged. We also thank the three anonymous reviewers who provided valuable assistance in improving the quality of this paper considerably.

References

ACTEW Corporation (2009), Appendix N: Greenhouse gas assessment, in *Murrumbidgee to Googong Water Transfer Project–Environmental Impact Statement*, Canberra.

Australian Bureau of Statistics (2008), *Population Projections: Australia 2006 to 2101*, 96 pp., Aust. Bur. of Stat., Canberra.

Australian Energy Market Operator (2014), *South Australian Fuel and Technology Report*, 50 pp, Aust. Energy Market Oper., Adelaide, South Australia.

Barjoveanu, G., I. Comandaru, G. Rodriguez-Garcia, A. Hospido, and C. Teodosiu (2014), Evaluation of water services system through LCA. A case study for Iasi City, Romania, *Int. J. Life Cycle Assess.*, *19*(2), 449–462, doi:10.1007/s11367-013-0635-8.

Beh, E. H. Y., G. C. Dandy, H. R. Maier, and F. L. Paton (2014), Optimal sequencing of water supply options at the regional scale incorporating alternative water supply sources and multiple objectives, *Environ. Modell. Software*, *53*, 137–153, doi:10.1016/j.envsoft.2013.11.004.

Cai, X. M., D. C. McKinney, and L. S. Lasdon (2002), A framework for sustainability analysis in water resources management and application to the Syr Darya Basin, *Water Resour. Res.*, *38*(6), doi:10.1029/2001WR000214.

Canadian Government (2011), National inventory report 1990–2009, greenhouse gas sources and sinks in Canada—The Canadian Government's submission to the UN framework convention on climate change, Part 3, *Rep. En81-4/2009E-PDF*, 105 pp., Environ. Can., Quebec.

Chong, J., J. Herriman, S. White, and D. Campbell (2009a), *Review of Water Restrictions*, vol. 1, *Review and Analysis*, 31 pp., Inst. for Sustainable Futures, ACIL Tasman Pty Ltd., Sydney, N. S. W., Australia.

Chong, J., J. Herriman, S. White, and D. Campbell (2009b), *Review of Water Restrictions*, vol. 2, *Appendices*, 31 pp., Inst. for Sustainable Futures, ACIL Tasman Pty Ltd., Sydney, N. S. W., Australia.

Clarke, J. M., P. H. Whetton, and K. J. Hennessy (2011), Providing application-specific climate projections datatsets: CSIRO's Climate Futures Framework, in *MODSIM2011, 19th International Congress on Modelling and Simulation*, edited by F. Chan, D. Marinova, and R. Anderssen, pp. 2683–2690, Modell. and Simul. Soc. of Aust. and N. Z., Canberra.

Deb, K., A. Pratap, S. Agarwal, and T. Meyarivan (2002), A fast and elitist multiobjective genetic algorithm: NSGA-II, *IEEE Trans. Evol. Comput.*, *6*(2), 182–197, doi:10.1109/4235.996017.

Department of Industry, Innovation, Climate Change, Science, Research, and Tertiary Education (2013), *Australian National Greenhouse Accounts*, 84 pp., Aust. Gov., Canberra.

Foster, V., and D. Bedrosyan (2014), Understanding CO_2 emissions from the global energy sector, *Rep. 85126*, 4 pp., Live Wire, World Bank Open Knowledge Repository, Wash.

Government of South Australia (2009), *Water for Good—A Plan to Ensure Our Water Future to 2050*, 190 pp., Gov. of South Aust., Adelaide.

Herstein, L., Y. Filion, and K. Hall (2009), Evaluating environmental impact in water distribution system design, *J. Infrastruct. Syst.*, *15*(3), 241–250, doi:10.1061/(ASCE)1076-0342(2009)15:3(241).

Herstein, L. M., and Y. R. Filion (2011), Life-cycle assessment of common water main materials in water distribution networks, *J. Hydroinf.*, *13*(3), 346–357, doi:10.2166/hydro.2010.127.

Herstein, L. M., Y. R. Filion, and K. R. Hall (2011), Evaluating the environmental impacts of water distribution systems by using EIO-LCA-based multiobjective optimization, *J. Water Resour. Plann. Manage.*, *137*(2), 162–172, doi:10.1061/(ASCE)WR.1943-5452.0000101.

Kasprzyk, J., P. Reed, B. Kirsch, and G. Characklis (2009), Managing population and drought risks using many-objective water portfolio planning under uncertainty, *Water Resour. Res.*, *45*, W12401, doi:10.1029/2009WR008121.

Kasprzyk, J., P. Reed, G. Characklis, and B. Kirsch (2012), Many-objective de Novo water supply portfolio planning under deep uncertainty, *Environ. Modell. Software*, *34*, 87–104, doi:10.1016/j.envsoft.2011.04.003.

Kasprzyk, J., S. Nataraj, P. Reed, and R. Lempert (2013), Many objective robust decision making for complex environmental systems undergoing change, *Environ. Modell. Software*, *42*, 55–71, doi:10.1016/j.envsoft.2012.12.007.

Keedwell, E., and S. T. Khu (2006), A novel evolutionary meta-heuristic for the multi-objective optimization of real-world water distribution networks, *Eng. Optim.*, *38*(3), 319–336, doi:10.1080/03052150500476308.

Lundie, S., G. M. Peters, and P. C. Beavis (2004), Life cycle assessment for sustainable metropolitan water systems planning, *Environ. Sci. Technol.*, *38*(13), 3465–3473, doi:10.1021/es034206m.

Maier, H. R., F. L. Paton, G. C. Dandy, and J. Connor (2013), Impact of drought on Adelaide's water supply system: Past, present and future, in *Drought in Arid and Semi-Arid Environments: A Multi-Disciplinary and Cross-Country Perspective*, edited by K. Schwabe et al., pp. 41–62, Springer, Dordrecht, Netherlands.

Miller, L., A. Ramaswami, and R. Ranjan (2013), Contribution of water and wastewater infrastructures to urban energy metabolism and greenhouse gas emissions in cities in India, *J. Environ. Eng.*, *139*(5), 738–745, doi:10.1061/(ASCE)EE.1943-7870.0000661.

Mortazavi, M., G. Kuczera, and L. Cui (2012), Multiobjective optimization of urban water resources: Moving toward more practical solutions, *Water Resour. Res.*, *48*, W03514, doi:10.1029/2011WR010866.

National Research Council (2009), Informing decisions in a changing climate, in *Panel on Strategies and Methods for Climate-Related Decision Support, Committee on the Human Dimensions of Global Change*, 188 pp., Div. of Behav. and Soc. Sci. and Educ., The Natl. Acad. Press, Washington, D. C.

Paton, F. L., H. R. Maier, and G. C. Dandy (2013), Relative magnitudes of sources of uncertainty in assessing climate change impacts on water supply security for the southern Adelaide water supply system, *Water Resour. Res.*, *49*, 1643–1667, doi:10.1002/wrcr.20153.

Paton, F. L., G. C. Dandy, and H. R. Maier (2014), Integrated framework for assessing urban water supply security of systems with non-traditional sources under climate change, *Environ. Modell. Software*, *60*(10), 302–319, doi:10.1016/j.envsoft.2014.06.018.

Piratla, K., S. Ariaratnam, and A. Cohen (2012), Estimation of emissions from the life cycle of a potable water pipeline project, *J. Manage. Eng.*, *28*(1), 22–30, doi:10.1061/(ASCE)ME.1943–5479.0000069.

Rambaud, S. C., and M. J. M. Torrecillas (2005), Some considerations on the social discount rate, *Environ. Sci. Policy*, *8*(4), 343–355, doi:10.1016/j.envsci.2005.04.003.

Reed, P., B. S. Minsker, and D. E. Goldberg (2003), Simplifying multiobjective optimization: An automated design methodology for the nondominated sorted genetic algorithm-II, *Water Resour. Res.*, *39*(7), 1196, doi:10.1029/2002WR001483.

Reed, P., D. Hadka, J. Herman, J. Kasprzyk, and J. Kollat (2013), Evolutionary multiobjective optimization in water resources: The past, present, and future, *Adv. Water Resour.*, *51*, 438–456, doi:10.1016/j.advwatres.2012.01.005.

Roshani, E., S. P. MacLeod, and Y. R. Filion (2012), Evaluating the impact of climate change mitigation strategies on the optimal design and expansion of the amherstview, Ontario, water network: Canadian case study, *J. Water Resour. Plann. Manage.*, *138*(2), 100–110, doi:10.1061/(ASCE)WR.1943-5452.0000158.

Rothausen, S. G. S. A., and D. Conway (2011), Greenhouse-gas emissions from energy use in the water sector, *Nat. Clim. Change*, *1*(4), 210–219, doi:10.1038/nclimate1147.

Sahely, H. R., and C. A. Kennedy (2007), Water use model for quantifying environmental and economic sustainability indicators, *J. Water Resour. Plann. Manage.*, *133*(6), 550–559, doi:10.1061/(ASCE)0733-9496(2007)133:6(550).

Sahely, H. R., C. A. Kennedy, and B. J. Adams (2005), Developing sustainability criteria for urban infrastructure systems, *Can. J. Civ. Eng.*, *32*(1), 72–85, doi:10.1139/l04-072.

Slagstad, H., and H. Brattebø (2014), Life cycle assessment of the water and wastewater system in Trondheim, Norway—A case study, *Urban Water J.*, *11*(4), 323–334, doi:10.1080/1573062x.2013.795232.

Stokes, C. S., A. R. Simpson, and H. R. Maier (2014), The cost-greenhouse gas emission nexus for water distribution systems including the consideration of energy generating infrastructure: An integrated conceptual optimization framework and review of literature, *Earth Perspect.*, *1*, 9, doi:10.1186/2194-6434-1-9.

Stokes, J., and A. Horvath (2006), Life cycle energy assessment of alternative water supply systems, *Int. J. Life Cycle Assess.*, *11*(5), 335–343, doi:10.1065/lca2005.06.214.

Stokes, J. R., and A. Horvath (2009), Energy and air emission effects of water supply, *Environ. Sci. Technol.*, *43*(8), 2680–2687, doi:10.1021/es801802h.

Weitzman, M. L. (2001), Gamma discounting, *Am. Econ. Rev.*, *91*(1), 260–271, doi:10.1257/aer.91.1.260.

Whetton, P., K. Hennessy, J. Clarke, K. McInnes, and D. Kent (2012), Use of representative climate futures in impact and adaptation assessment, *Clim. Change*, *115*, 433–442, doi:10.1007/s10584-012-0471-z.

Wilby, R. L., and S. Dessai (2010), Robust adaptation to climate change, *Weather*, *65*(7), 180–185, doi:10.1002/wea.543.

Wu, W., A. Simpson, and H. Maier (2009), Single-objective versus multi-objective optimization of water distribution systems accounting for greenhouse gas emissions by carbon pricing, *J. Water Resour. Plann. Manage.*, *36*(5), 555–565, doi:10.1061/(ASCE)WR.1943-5452.0000072.

Wu, W., A. Simpson, and H. Maier (2010), Accounting for greenhouse gas emissions in multiobjective genetic algorithm optimization of water distribution systems, *J. Water Resour. Plann. Manage.*, *136*(2), 146–155, doi:10.1061/(ASCE)WR.1943-5452.0000020.

Wu, W., A. Simpson, H. Maier, and A. Marchi (2012), Incorporation of variable-speed pumping in multiobjective genetic algorithm optimization of the design of water transmission systems, *J. Water Resour. Plann. Manage.*, *138*(5), 543–552, doi:10.1061/(ASCE)WR.1943-5452.0000195.

Wu, W., H. Maier, and A. Simpson (2013), Multiobjective optimization of water distribution systems accounting for economic cost, hydraulic reliability, and greenhouse gas emissions, *Water Resour. Res.*, *49*(3), 1211–1225, doi:10.1002/wrcr.20120.